Proceedings of the 11th ICPMG 2026
11th International Conference on Physical Modelling in Geotechnics
8-12 June 2026, Zurich, Switzerland

Research on the installation mechanism of helical anchors in layered clay

L. Wang, Z. Ji
Tianjin University, Tianjin, China, lewang_1895@tju.edu.cn, zhaobinji2025@163.com

J. He
China Harbour Engineering Company Limited, Beijing, China, jbhe@chec.bj.cn

Y. Xu
Tianjin Research Institute for Water Transport Engineering, Ministry of Transport, Tianjin, China, yunlongxu1992@163.com

D. Hao
Northeast Electric Power University, Jilin, China, haodongxue2005@126.com

W. Hu
Hunan University of Science and Technology, Xiangtan, China, yilukuangben1982@163.com

Z. Shen
South China University of Technology, Guangzhou, China, shenzhichao@scut.edu.cn

C. Zhang
Hebei University of Science and Technology, Shijiazhuang, China, zhangchunhui789@163.com

Y. Tian
The University of Melbourne, Melbourne, Australia, yinghui.tian@unimelb.edu.au

L. Zhang, C. Li
Tianjin University, Tianjin, China, 202420509@tju.edu.cn, lch2025@tju.edu.cn

ABSTRACT: The successful installation of large-scale offshore helical anchors has become a critical factor in determining their practical applicability in floating wind power projects. However, most existing research on helical anchor installation has focused on homogeneous soil conditions, without adequately accounting for the complexity introduced by realistic layered soil. To address this gap, a CEL-based large-deformation numerical framework tailored for soft-over-stiff double-layer clay was developed. This model simulates the installation of helical anchors in soft-over-stiff clay, characterizing the load-transfer and the depth-dependent variations in installation torque and vertical force. To further elucidate the mechanisms governing force and torque development, the contributions of individual helical anchor components were quantified, and the surrounding soil flow behavior during penetration was analyzed. These findings elucidate the installation of helical anchors in layered clay, thereby providing insights for future research on layered soils.

1 INTRODUCTION

1.1 Research background

Floating offshore wind power has become an important foundation solution for deep-sea renewable energy development (Chu and Majumdar, 2012). The mooring foundation is one of the most critical components of floating wind turbine systems, and its performance is directly tied to the overall safety and reliability of the platform. Currently adopted mooring foundations include gravity-based foundations, suction anchors, drag-embedded plate anchors, and helical anchors. Among these options, helical anchors exhibit considerable potential for large-scale offshore applications owing to their advantages such as rapid installation (Al-baghdadi et al., 2017), low noise, straightforward retrieval (Ding et al., 2019) and excellent pull-out resistance (Cerfontaine et al.,2023). However, the installation of helical anchors involves highly nonlinear soil-structure interactions. In practical offshore environments, seabed soils typically exhibit pronounced stratification, and their strength varies strongly with depth, which can substantially affect the installation resistance of helical anchors. At present, the installation mechanism of helical anchors in layered clay remains insufficiently clarified, making it difficult to accurately predict the installation torque and force. Therefore, a systematic and rigorous investigation of the installation of helical anchors in layered soils is crucial for advancing their application in floating wind turbine mooring systems.

1.2 Literature Review

The distinctive mechanical behavior and installation processes of helical anchors have made them a prominent research topic in geotechnical engineering. To date, numerous studies based on model tests (Nagai et al., 2018; Li et al., 2022; Ullah et al., 2024), theoretical analyses (Todeshkejoei, 2018; Li et al., 2022), and numerical simulations (Pucker and Grabe, 2012; Yu et al., 2022) have primarily focused on the prediction of installation loads in homogeneous clay or sand. However, in practical offshore sites such as the South China Sea (Tamburini et al., 2003) and the Northwest Shelf of Australia (Thiry, 2000), the seabed generally comprises layered clay exhibiting pronounced strength variations with depth. The core difference in the installation mechanisms of helical anchors between layered clay and homogeneous soil lies in the force characteristics and soil disturbance behaviors at the soil layer interface, and this difference directly alters the engineering prediction and design logic:① The installation torque and vertical force of helical anchors in homogeneous soil show a stable growth trend with depth, while both undergo significant abrupt changes at the soft-stiff soil interface in layered clay, when penetrating from soft soil to stiff soil, the torque and vertical force exhibit a stepwise sharp increase, and a steep decrease may occur when transitioning from stiff soil to soft soil. This mutation is a core feature that requires key attention in engineering design (Zhao et al., 2023; Ullah et al., 2024);② On the one hand, the upper soil layer is entrained into the lower layer during the rotational penetration of the helical blades, triggering the expansion of the soil shear zone and the transformation of failure modes at the interface (Ullah et al., 2024; Li et al., 2022); on the other hand, the force mode on the upper and lower surfaces of the helical blades at the interface fluctuates drastically, with alternating changes of force on the upper surface, force on the lower surface, or bidirectional force. These two factors collectively lead to the mutation of installation force and torque (Yu et al., 2022). However, traditional prediction models based on homogeneous soil fail to capture this feature. Therefore, it is necessary to specifically introduce an interface correction factor in engineering design to avoid underestimating the resistance requirement at the interface and improve prediction accuracy (Al-Baghdadi et al., 2017). Accordingly, a systematic and mechanistically oriented investigation into the evolution of load transfer along different components and the associated soil flow mechanisms during penetration is essential for enhancing the accuracy of installation load prediction and the reliability assessment of in-service performance.

1.3 Research Methodology

To realistically simulate the installation process of helical anchors in layered clay, a large-deformation numerical framework based on the Coupled Eulerian-Lagrangian (CEL) approach was developed. The CEL method (Dassault Systèmes, 2016) effectively circumvents the severe mesh distortion typical of conventional finite element analyses, thereby enabling accurate simulation of large soil deformation and flow induced by the continuous anchor rotation and penetration. This study considers a representative soft-over-stiff double-layer clay profile, with undrained shear strength of S_{u1}=10 kPa for the upper layer and S_{u2}=100 kPa for the lower layer. The modeling procedure follows a layered logic framework (Wang et al., 2025). Subsequently, this study analyzes the installation torque and force, the load-transfer evolution among different components of the helical anchor, and the soil flow behavior around the anchor, thereby elucidating the characteristic installation mechanisms in layered clay with emphasis on interface-controlled resistance transition.

2 NUMERICAL SIMULATION OF HELICAL ANCHORS IN LAYERED CLAY

2.1 Verification of the CEL model

The numerical simulations were conducted using Abaqus/Explicit. Prior to developing the primary model, the CEL modeling approach was verified to ensure the robustness of the modeling strategy and the validity of the numerical results. The validation was carried out by comparing the present CEL model with the numerical results reported by Ullah et al. (2024). As shown in Figure 1, the normalized torque-depth response obtained from the present simulation shows good agreement with the CEL simulations of Ullah et al. (2024). The minor discrepancies may be attributed to differences in output intervals and post-processing procedures. This comparison supports the reliability and suitability of the CEL modeling methodology adopted in this study.

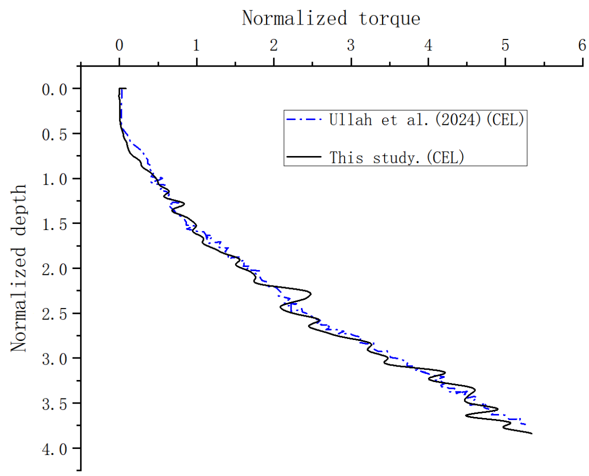

Figure 1. Validation of the CEL model against published results.

2.2 Modeling details

As illustrated in Figure 2, the soil domain was modeled as an Eulerian continuum, while the helical anchor was idealized as a Lagrangian rigid body. To ensure numerical stability and prevent soil heaving from compromising computational stability during installation, a void layer with a thickness of 1*D* (where *D* denotes the helix diameter) was introduced above the Eulerian domain. To minimize boundary effects, the soil domain was assigned radial and vertical dimensions of 8*D* and 14*D*, respectively, which accommodates an installation depth of 8*D*. The boundary conditions were specified as follows: the bottom surface was fixed in all directions, while the side boundaries were constrained in the radial and circumferential directions but allowed to move vertically. The soil and anchor were discretized using EC3D8R Eulerian elements and C3D10M tetrahedral elements, respectively. To enhance computational accuracy in the contact region, the mesh was refined within a radial distance of 1*D* from the anchor axis. The minimum mesh size was set to *D*/48 (Kwon et al., 2019), and the mesh gradually coarsened with increasing distance from the anchor axis. Vertically, the mesh density was increased only within the 8*D* penetration zone of the helical anchor. The entire model contained approximately 1,163,251 elements. The detailed geometric and mechanical parameters for the soil layers and the helical anchor are summarized in Table 1 and Table 2, respectively.

The numerical analysis consisted of two stages: initial geostatic stress equilibrium was first established, followed by anchor installation to a depth of 8*D* with a rotational velocity V_r= 6.28 rad/s and a vertical velocity V_v= 0.64 m/s. The soil-anchor interaction was modeled using a penalty contact model, allowing for separation after contact, and the tangential response was followed by the Coulomb friction law. A friction coefficient of 1.0 was adopted, representing a fully rough clay–steel contact condition.

Table 1. Dimensions and parameters of the soil.

Parameter	Upper layer of clay H_1	Lower layer of clay H_2	void layer H_0
Height *H*(m)	8	18	2
Soil radius R_s(m)		8	
Undrained shear strength S_u(KPa)	10	100	/
Young's modulus *E*(GPa)	0.005	0.05	/
Effective unit weight γ(kN/m³)	10		/
Poisson ratio ν	0.49		/

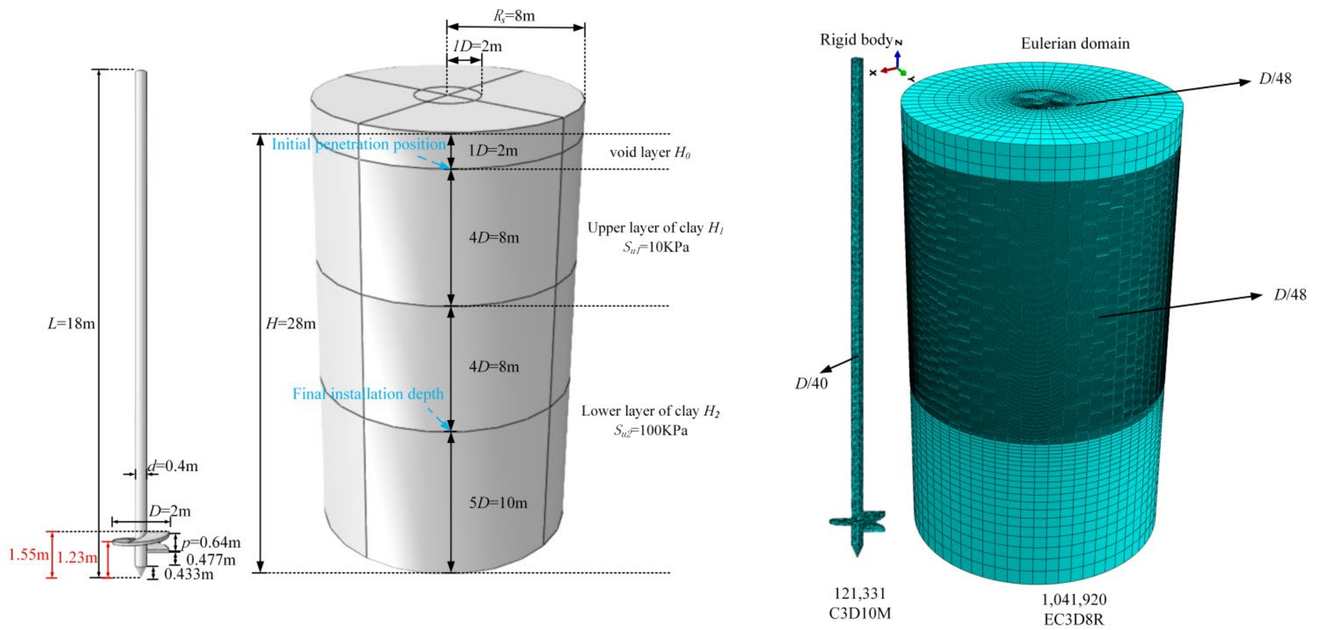

Figure 2. Schematic of the CEL modeling framework and mesh configuration.

Table 2. Dimensions and parameters of the helical anchor.

Parameter	Value	Parameter	Value
Shaft diameter d(m)	0.4	Helix blade diameter D(m)	2
Length L(m)	18	Helix pitch p(m)	0.64
Cone angle β(°)	60	Pile density p(kg/m³)	7850
Number of helixes n	1	Poisson ratio v	0.3
Plate thickness t(m)	0.1	Young's modulus E(GPa)	210

3 RESULTS AND DISCUSSION

3.1 Installation torque and vertical force

Figure 3(a) and (b) illustrate the variation of installation torque and vertical force with penetration depth. It is evident that significant differences exist in both installation torque and vertical force between homogeneous soil and layered soil conditions, especially at the interface between the soil layers where both exhibit a marked increase. During the initial stage (0 to 0.91 m), when the helical anchor first contacts the soil, both installation torque and vertical force are relatively small. As penetration proceeds from 0.91 m to 1.55 m, the helical blades begin to engage the soil, leading to an accelerated increase in installation torque. Between 1.55 m to 8 m penetration, with the anchor fully embedded in the upper clay, both torque and vertical force exhibit stable growth with depth. When penetrating from 8 m to 10 m, the anchor transitions from soft to stiff clay. Initially, the cone tip comes into contact with the underlying stiff layer. Subsequently, when the penetration depth reaches 8.91 m, the helical blades begin to engage the underlying soil; as penetration continues to 9.55 m, the helical blades fully enter the underlying soil; during this process, both torque and vertical force rise sharply. From 10 m to 11 m, the installation torque continues to rise, whereas the vertical force slightly decreases, which can be attributed to the full engagement of the helical blades within the stiffer clay layer and the development of stronger confinement effects. A temporary reduction in installation torque is observed when the penetration depth reaches 11–12 m, reflecting the adjustment of the helical anchor to the mechanical properties of the stiff layer. Meanwhile, a noticeable increase in vertical force occurs as the soil reaction on the upper helix surface approaches a stable state. The continued engagement of the helical blades and the stiff soil layer further intensifies the increase in the vertical force. Finally, during 12 m to 16 m, both installation torque and vertical force stabilize and exhibit a steady growth trend.

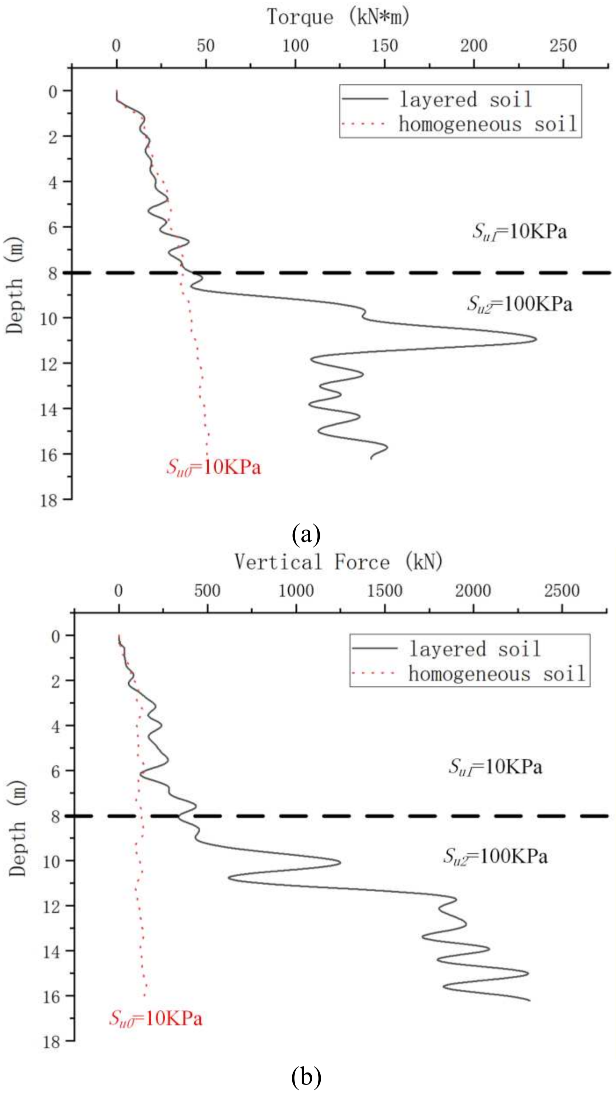

Figure 3. Results of installation torque and vertical force varying with depth. (a) Torque varies with depth; (b) The vertical force varies with depth.

3.2 Vertical force distribution among anchor components

To elucidate the load transfer mechanism, the vertical forces acting on different structural components of the helical anchor during installation were quantified. The anchor was divided into four regions: the cone, the shaft, and the upper and lower surfaces of the helix. Owing to the soil-anchor interactions during installation, the upper surface of the helix is mainly subjected to a downward compressive reaction force, whereas the remaining three regions primarily experience upward resistance. The values of the vertical forces are plotted in Figure 4. The helical blade consistently accounts for more than 70% of the total vertical resistance throughout the installation process. During the critical penetration stage spanning 8–12 m, which involves the transition into the stiff clay layer and subsequent stabilization, fluctuations in total vertical force are governed predominantly by the reactions on the upper and lower helical surfaces. This behavior, as shown in Figure 4, exhibits strong consistency with the installation torque and vertical force evolution presented in Figure 3. This indicates that blade–soil interaction governs the installation resistance response in layered clay.

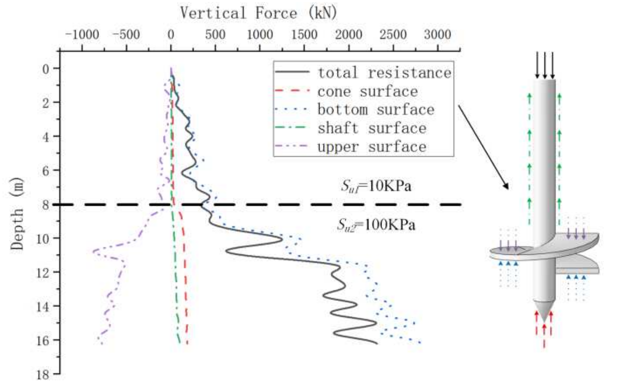

Figure 4. Vertical forces distribution along the helical anchor with depth.

3.3 Soil flow situation

To elucidate the soil flow mechanism during installation, the distribution of soil displacement around the anchor was analyzed at penetration depths in the upper layer (4 m), the interface (9.23 m), and the lower layer (14 m), as shown in Figure 5(a)-(c). In the displacement contour, blue denotes regions with smaller displacement, where soil movement is approximately equal to the vertical displacement of the helical anchor; whereas red represents regions of larger soil movement, where the soil displacement is approximately 5-10 times the vertical displacement of the anchor. The results indicate that soil movement is consistently concentrated beneath the lower helix surface, with only limited soil migration occurring along the shaft. The extent and intensity of soil displacement evolve significantly with penetration depth, and greater soil mobilization corresponds to higher installation torque and vertical force. Consequently, the observed soil flow characteristics show clear correlation with the variations in installation torque and vertical force with depth presented in Figure 3.

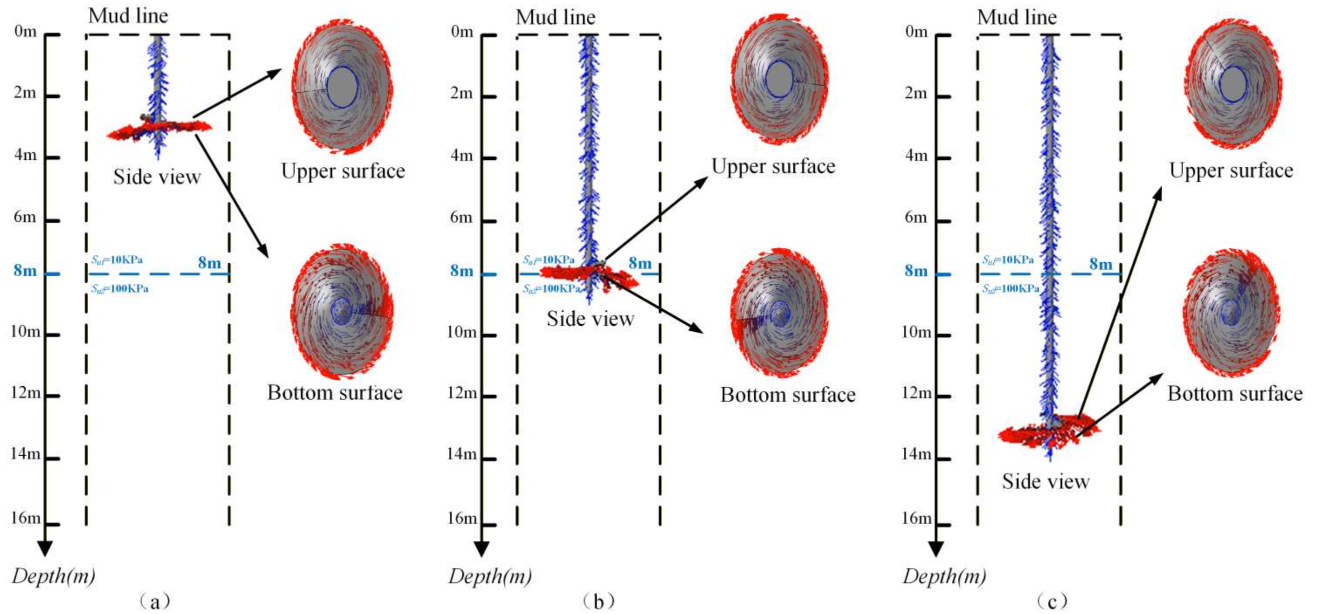

Figure 5. Soil flow situation. (a) Depth=4m; (b) Depth=9.23m;(c) Depth=14m.

4 CONCLUSIONS

This study examines the installation response of helical anchors in soft–stiff double-layer clay using the coupled Eulerian–Lagrangian (CEL) method, with emphasis on prediction and design implications, and the key conclusions are as follows:

(1) The installation torque and vertical force of helical anchors in layered clay exhibit a pronounced stepwise transition at the soft-stiff interface, with the mutation depth ranging from the cone tip contacting the stiff clay layer to the helical blades fully penetrating into the stiff clay layer (8-9.55 m in this study). Within this interface transition zone, conventional homogeneous-soil-based prediction approaches may underestimate installation resistance; therefore, an interface correction factor should be introduced within this depth range in engineering predictions to avoid underestimation of resistance;

(2) The helical blades are the core components contributing to vertical resistance (accounting for more than 70% of the total vertical force), and the vertical force fluctuation at the interface is mainly dominated by the difference in soil reaction forces on the upper and lower surfaces of the blades. This indicates that blade geometry and blade–shaft connection integrity play a critical role in structural safety during installation, and should therefore be emphasized in design.

The CEL numerical framework established in this study demonstrates the capability to capture interface-induced resistance transition in layered clay and provides a mechanistic basis for the installation design of helical anchors in layered clay. Future investigations incorporating multi-helix configurations and inclined penetration will further extend the applicability of the present findings.

ACKNOWLEDGEMENTS

The author would like to acknowledge the support from National Natural Science Foundation of China (No.52471294), the Project supported by the Natural Science Foundation of Hebei Province, China(No.E2023208053), and the Open Fund of the State Key Laboratory of Ocean Engineering (No. 2416).

REFERENCES

Al-Baghdadi, T., Davidson, C., Brown, M. J., Knappett, J. A., Brennan, A., Augarde, C., ... & Blake, A. (2017). CPT based design procedure for installation torque prediction for screw piles installed in sand. *In 8th Offshore Site Investigation and Geotechnics International Conference: 'Smarter Solutions for Future Offshore Developments'* (pp. 346-353). Society for Underwater Technology. https://doi.org/10.3723/OSIG17.346.

Cerfontaine, B., White, D., Kwa, K., Gourvenec, S., Knappett, J., & Brown, M. (2023). Anchor geotechnics for floating offshore wind: Current technologies and future innovations. *Ocean Engineering*, 279, 114327. https://doi.org/10.1016/j.oceaneng.2023.114327.

Chu, S., & Majumdar, A. (2012). Opportunities and challenges for a sustainable energy future. *Nature*, 488 (7411), 294-303. https://doi.org/10.1038/nature11475.

Dassault Systèmes (2016). Abaqus Analysis User's Manual. SIMULIA, Providence, RI.

Ding, H., Wang, L., Zhang, P., Liang, Y., Tian, Y., & Qi, X. (2019). The recycling torque of a single-plate helical pile for offshore wind turbines in dense sand. *Applied Sciences*, 9(19), 4105. https://doi.org/10.3390/app9194105.

Kwon, O., Lee, J., Kim, G., Kim, I., & Lee, J. (2019). Investigation of pullout load capacity for helical anchors subjected to inclined loading conditions using coupled Eulerian-Lagrangian analyses. *Computers and Geotechnics*, 111, 66-75. https://doi.org/10.1016/j.compgeo.2019.03.007.

Li, W., Deng, L., & Chalaturnyk, R. (2022). Centrifuge modeling of the behaviour of helical piles in cohesive soils from installation and axial loading. *Soils and Foundations*, 62(3), 101141. https://doi.org/10.1016/j.sandf.2022.101141.

Nagai, H., Tsuchiya, T., & Shimada, M. (2018). Influence of installation method on performance of screwed pile and evaluation of pulling resistance. *Soils and Foundations*, 58(2), 355-369. https://doi.org/10.1016/j.sandf.2018.02.006.

Pucker, T., & Grabe, J. (2012). Numerical simulation of the installation process of full displacement piles. *Computers and Geotechnics*, 45, 93-106. https://doi.org/10.1016/j.compgeo.2012.05.006.

Tamburini, F., Adatte, T., & Föllmi, K. B. (2003). Origin and nature of green clay layers, ODP Leg 184, South China Sea. *In Proceedings of the Ocean Drilling Program*, *Scientific Results* (Vol. 184, No. 1, p. 23). https://doi.org/10.2973/odp.proc.sr.184.206.2003.

Thiry, M. (2000). Palaeoclimatic interpretation of clay minerals in marine deposits: an outlook from the continental origin. *Earth-Science Reviews*, 49(1-4), 201-221. https://doi.org/10.1016/S0012-8252(99)00054-9.

Todeshkejoei, K. (2018). Mechanics of Screw Piles in Clay. PhD thesis, The University of Newcastle, Newcastle.

Ullah, S. N., & Hu, Y. (2020). Discussion: A review on the behaviour of helical piles as a potential offshore foundation system. *Marine Georesources & Geotechnology*, 38(9), 1121-1127. https://doi.org/10.1080/1064119X.2020.1729905.

Ullah, S. N., O'Loughlin, C., Hu, Y., & Hou, L. F. (2024). Torsional installation and vertical tensile capacity of helical piles in clay. *Géotechnique*, 74(12), 1360-1376. https://doi.org/10.1680/jgeot.22.00014.

Wang, L., Zhang, L., Chen, L., Huang, X., Zhang, C., Shen, Z., ... & Tian, Y. (2025, June). Numerical Analysis of Installation Mechanisms for Floating Wind Turbine Helical Anchors in Sand. *In International Conference on Offshore Mechanics and Arctic Engineering* (Vol. 88957, p. V006T10A008). American Society of Mechanical Engineers. https://doi.org/10.1115/OMAE2025-156765.

Yu, H., Zhou, H., Sheil, B., & Liu, H. (2022). Finite element modelling of helical pile installation and its influence on uplift capacity in strain softening clay. *Canadian Geotechnical Journal*, 59(12), 2050-2066. https://doi.org/10.1139/cgj-2021-0527.

Zhao, H., Wang, L., Sun, L. Q., Tian, Y. H., Reul, O., & Chen, Q. Z. (2023). Pile running in layered soils. China Ocean Engineering, 37(5), 829-841. https://doi.org/10.1007/s13344-023-0069-4.

Zhou, S., Zhou, M., Tian, Y., & Zhang, X. (2022). Numerical investigation of caisson with pad-eye stiffener installation into nonhomogeneous clay. *Applied Ocean Research*, 121, 103077. https://doi.org/10.1016/j.apor.2022.103077.